



## Calotropis procera as effective adsorbent for removal of malachite green dye: a comprehensive study

Rajvir Kaur, Harpreet Kaur\*

Department of Chemistry, Punjabi University, Patiala 147002, Punjab, India, Tel. +91 9463489248;  
email: preetjudge@yahoo.co.in (H. Kaur), Tel. +91 8872300538; email: srawrajvir021@gmail.com (R. Kaur)

Received 8 September 2016; Accepted 27 January 2017

### ABSTRACT

The present work is devoted to study the influence of various factors such as contact time, adsorbent dose, initial dye concentration, ionic concentration, pH, temperature and desorption for adsorption of malachite green (MG) on dried leaf powder of *Calotropis procera* (DPCP) and thereby to determine the kinetics of process by subjecting the data to various kinetic models, i.e., pseudo-first-order, pseudo-second-order, intra-particle diffusion and Elovich models. It has been observed that kinetic is best fitted to pseudo-second-order model. The adsorption data have been fitted with Langmuir, Freundlich, Temkin and Dubinin–Radushkevich isotherm models with maximum adsorption capacity 39.22 mg g<sup>-1</sup>. The thermodynamic studies of process confirm that process is spontaneous over the temperature range of 293.15–323.15 K. The whole studies have been monitored by UV–visible spectrophotometer. The prepared biomass has been characterized by X-ray fluorescence, X-ray diffraction, Brunauer–Emmett–Teller, scanning electron microscopy and Fourier transformer infrared studies. The results showed that abundant and eco-friendly nature of DPCP (without any pre-treatment) has been proven its potential application toward MG dye treatment.

*Keywords:* *Calotropis procera*; Eco-friendly; Cellulose; Malachite green; Water remediation

### 1. Introduction

*Calotropis procera* is an ayurvedic plant of family 'Asclepiadaceae' and is well known for its medicinal properties. This plant is found in most parts of the world in dry, sandy, alkaline soils, warm climate and is more common in south-western, central India and western Himalayans. The dried leaves are used as an expectorant and anti-inflammatory for the treatment of paralysis, rheumatic and joints pains [1,2]. In the present study, powder of dried leaves of plant due to its biodegradable and eco-friendly nature has been used to control the pollution due to dyes.

During recent years, water pollution is the major topic of concern all over the world. The increasing contamination of freshwater systems with thousands of industrial and chemical compounds (especially textile industry effluent) is one of

the key environmental problem worldwide. Textile industry produces a lot of wastewater, which contains many contaminants like: dyes, metals, salts, surfactants, etc., which may be added to improve dye adsorption onto the fibers. Because of their complex molecular structure and large sizes most of the dyes are considered non-oxidizable by conventional physico-chemical methods [3]. Cationic dye, malachite green (MG) is belonging to the triphenylmethane family and is widely used as fungicide, disinfectant and to color fabric products [4,5]. But literature reported [6,7] that MG is lethal to freshwater fish in both acute and chronic exposure, cytotoxic to mammalian cells which affect the liver, kidney, heart, eye, skin and increasing the risk of cancer. The day by day increasing demand for safe water requires effective and economical water treatment method due to limited aquatic resources [8]. Among the other reported methods [9], adsorption has been found to be the most efficient and widely accepted process for the wastewater treatment because of its simplicity of

\* Corresponding author.

design, technical feasibility and social acceptability [10,11]. Adsorption method has encouraged the development of new adsorbent, which are abundant in nature. Recently, with growing interest in finding new adsorbents for the removal of MG dye has developed paper industry sludge [12], *Azadirachta indica* [13], alkali-modified malted sorghum mash [14], chemically modified rice husk [15], activated carbon tea leaves [16], chemically modified breadnut peel [17], walnut shell [18] and activated carbon prepared from bamboo [19]. But most of these adsorbents are in the form of activated carbon and chemically modification with limited adsorption capacities, high cost, regeneration and disposal problems. To the best of our knowledge, the use of *Calotropis procera* waste as adsorbent for the removal of MG dye from water has not been yet reported and does not cause any secondary pollutant.

The main objective of this work is to develop an efficient and cost-effective method toward adsorption of dye. The various constituents present in dried leaf powder of *Calotropis procera* (DPCP) and its surface morphology has been determined by X-ray fluorescence (XRF), X-ray diffraction (XRD), Brunauer–Emmett–Teller (BET), Fourier transformer infrared (FTIR) and scanning electron microscope (SEM) techniques. Effect of contact time, adsorbent amount, initial dye concentrations, pH and ionic strength on the removal has been examined to optimize parameters for the highest efficiency of the process. Adsorption capacity data have been proven the effectiveness of DPCP with other adsorbents. Kinetics studies for the removal of MG on DPCP have been elaborated under optimized conditions to study the adsorption isotherms, kinetics, thermodynamics and regeneration of the adsorption process.

## 2. Materials and method

### 2.1. Chemicals

Water has been purified by adding potassium permanganate with a pellet of potassium hydroxide and then fractionally distilled. Stock solution of 1,000 mg L<sup>-1</sup> (MG) has been prepared in deionized water. The resulting stock solution has been stored in the air tight glass flasks. The absorbance of MG has been measured at maximum wavelength 618 nm, using Shimadzu UV-1800, UV-visible spectrophotometer. All other chemicals used for experiments such as sodium hydroxide, hydrochloric acid and sodium chloride have been of analytical grade and used as received.

### 2.2. Preparation of the biosorbent

The leaves of *Calotropis procera* has been collected from Patiala city, Punjab, India. These leaves have been washed with tap water, finally with deionized water to remove dirt particles and dried at 100°C for 24 h, crushed in grinder and sieved through micron sized mesh. The DPCP has been stored in an airtight container. Thus, DPCP as an adsorbent has been prepared in a very economical and easy way without any treatment process.

### 2.3. Batch biosorption experimental procedure

All adsorption experiments have been carried out by agitating 0.5 g of DPCP with 100 mL of dye solution

of desired concentration and pH, at different temperature using rotary orbital shaker at 250 rpm. The sample has been withdrawn at predetermined time intervals then centrifuged at 2,000 rpm for 10 min. The absorbance of supernatant solution has been determined spectrophotometrically by monitoring the absorbance at 618 nm. The pH of the solution has been adjusted using 0.1 N NaOH and 0.1 N HCl and measured with digital Elico pH meter. The batch adsorption studies have been conducted to study the effect of different parameters such as: contact time (5–120 min), adsorbent amount (0.1–1.1 g), initial dye concentrations (25–150 mg L<sup>-1</sup>), pH (2–10) and temperature (293.15–323.15 K). The effect of electrolyte has been investigated for 100 mL of MG dye solution (100 mg L<sup>-1</sup>) at optimized conditions. The experimental data have been subjected to isotherms (Langmuir, Freundlich, Temkin and Dubinin–Radushkevich isotherm models) and kinetics models (pseudo-first-order, pseudo-second-order, intra-particle diffusion and Elovich). The amount of equilibrium adsorption  $q_t$  (mg g<sup>-1</sup>) and percentage removal of MG have been calculated by using the following equations:

$$q_t = (C_0 - C_e)V / W \quad (1)$$

$$\text{Removal (\%)} = (C_0 - C_e) / C_0 \times 100 \quad (2)$$

where  $C_0$  and  $C_e$  are the initial and equilibrium concentrations of MG in solution (mg L<sup>-1</sup>),  $V$  is the volume of the solution (L) and  $W$  is the mass of dry adsorbent (g).

## 3. Results and discussion

### 3.1. Characterization

#### 3.1.1. XRF elemental analysis

XRF spectrometry (WD-XRF spectrometer Model-S8 TIGER Bruker) has been used to determine the elemental composition of the DPCP and the results are listed in Table 1. One distinctive observation in the XRF analysis is C<sub>6</sub>H<sub>10</sub>O<sub>5</sub> cellulose is the major component present which is polysaccharide consisting of a linear chain of several hundred to many thousands of β(1 → 4) linked D-glucose units, while the remaining elements in traces. There is a possibility that cationic dye molecules are replacing these metal ions with their partial hydration through ion exchange [20,21]. The high cellulose content as fiber has been proven to be of advantage for use as economical adsorbent in adsorption method [22].

#### 3.1.2. XRD studies

The powder XRD pattern of *Calotropis procera* adsorbent has been recorded using X-Pert Pro X-ray diffractometer equipped with a Cu Kα radiation source (λ = 0.15418 nm) operated at 45 kV and a current 40 mA. Fig. 1 represents the diffraction spectrum at 22° and 15°, which showed the existence of cellulose [23]. The highest intensity of the peak at 22° due to the  $hkl$  plane (002) confirms the amorphous nature of the adsorbent [24,25].

### 3.1.3. Brunauer–Emmett–Teller

The BET surface area of the prepared adsorbent was measured through  $N_2$  adsorption at 77 K in the relative pressure 0.99 using BET surface area analyzer (Autosorb-1C Quantachrome). The BET surface area of DPCP has been found to be  $0.339 \text{ m}^2 \text{ g}^{-1}$ .

### 3.1.4. FTIR analysis

FTIR spectrum of MG consist of characteristic peaks at  $1,720 \text{ cm}^{-1}$ , which may correspond to C=N stretching frequency of amine in quinoid structure and one peak at  $1,368 \text{ cm}^{-1}$  C–N stretch due to aromatic amine. The other bands appear at  $1,585, 1,513, 1,477$  and  $1,446 \text{ cm}^{-1}$  (may correspond to C=C aromatic stretching);  $1,612 \text{ cm}^{-1}$  (may be due to tertiary substituted C=C); and  $3,053$  and  $2,921 \text{ cm}^{-1}$  (may be due to C–H stretching of aromatic and methyl group, respectively). FTIR spectrum of DPCP before adsorption consist of peaks at  $3,390, 2,926, 1,644, 1,324, 1,154, 1,101$  and  $1,066$ , which may be attributed to O–H stretching vibrations, asymmetric

C–H stretching, OH bending vibrations, C–O groups on the biomass surface, anti-symmetric bridge C–OR–C stretching (cellulose), anhydroglucose ring and C–OR stretching of cellulose, respectively [8]. However, FTIR spectrum of DPCP after the dye adsorption (Fig. 2(b)), consist of peaks at  $3,390, 2,130, 1,644, 1,424, 1,324, 1,154, 896$  and  $640 \text{ cm}^{-1}$ , which are presented at slightly shifted positions and a new peak is observed at  $1,732 \text{ cm}^{-1}$ , which may correspond to C=N stretching of MG (adsorbed on DPCP). This band is present at shifted position which suggested the interactions of dye with the functional groups of adsorbent.

### 3.1.5. Scanning electronic micrographic studies

The morphological characterization of the adsorbent and MG dye adsorbed onto adsorbent has been examined by JEOL model JSM6610 SEM at 30 kV. For SEM observation, particles of the adsorbent have been dispersed onto carbon tape and coated with gold using a sputter coater to prevent charge accumulation on the sample. As seen from Fig. 3(a), DPCP has a porous and rough surface. Thus, there is a good possibility for adsorption of dye into its pores. Fig. 3(b) shows that surface of the adsorbent becomes smooth after adsorption of MG because pores are covered by dye.

Table 1  
Characterization of elements of DPCP by XRF

S.No.	Elements	Results (%)
1	$C_6H_{10}O_5$	96.10
2	Na	0.20
3	Mg	0.54
4	Al	0.03
5	Si	0.13
6	P	0.18
7	S	0.29
8	Cl	0.07
9	K	0.03
10	Ca	2.31
11	Ti	0.002
12	Fe	0.03
13	Ni	0.0019
14	Cu	0.0015
15	Zn	0.03
16	Mn	0.02
17	Sr	0.01
18	Ru	0.0013
19	Mo	0.0009
20	U	0.0008

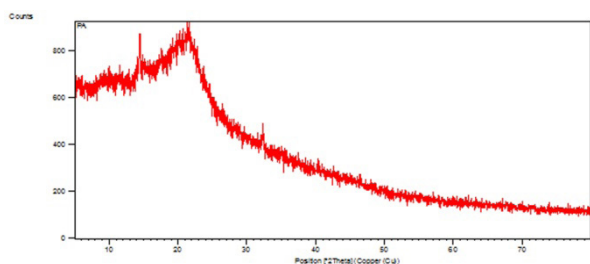


Fig. 1. X-ray diffraction of DPCP.

### 3.2. Effect of contact time and initial concentration of MG

The effect of contact time with dye concentration is an essential parameter in the adsorption process as the data will allow to confirm the length of agitation time to achieve the equilibrium. The time dependent behavior of adsorption of MG onto DPCP has been studied over the range of initial dye concentrations ( $25\text{--}150 \text{ mg L}^{-1}$ ) along with  $0.5 \text{ g}$  of DPCP at  $303.15 \text{ K}$ . The variation of adsorption capacity as a function of contact time has been fast initially and then become slower (Fig. 4(a)). The maximum uptake has been achieved in  $60 \text{ min}$  for adsorption of MG at various initial concentrations ( $25\text{--}150 \text{ mg L}^{-1}$ ). The adsorption rate after this phase has been increased slowly, which means the attainment of equilibrium state. The rapid adsorption rate within short equilibrium time indicates a high affinity between the DPCP and MG, which may be due to the availability of large specific surface area and pore volume of the adsorbent [26]. But with increase of contact time, more and more dye particles get adsorbed over the surface and free surface for adsorption decreases, and hence the rate of adsorption decreases.

The variation of MG removal and adsorption capacity as a function of initial dye concentration indicates (Fig. 4(b))

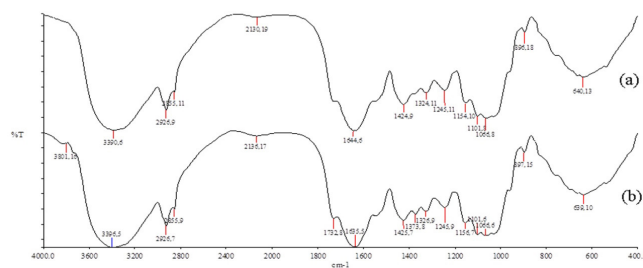


Fig. 2. FTIR spectra of: (a) DPCP before adsorption and (b) after adsorption of MG.

that at low concentration the ratio of the initial number of dye molecules to the available surface area is low and at higher concentration, it is more [27], which result in increases in adsorption capacity of DPCP 4.78–26.93 mg g<sup>-1</sup> and decrease of percentage removal from 95.50% to 89.75% at concentration range of 25–150 mg L<sup>-1</sup>.

3.3. Effect of amount of adsorbent

The effect of amount of DPCP on MG removal has been investigated to optimize the minimum dosage required for a given concentration of the adsorbate to attain the maximum uptake capacity. Experiments have been carried out by varying the amount of adsorbent (0.1–1.1 g) in the 100 mL dye solution with an initial dye concentration of 100 mg L<sup>-1</sup> at 303.15 K for 60 min. The percentage removal has been increased from 79.75% to 97.00% with increase in amount of adsorbent from 0.1 to 1.1 g. As depicted from Fig. 5, the rate of removal has been increased due to increase in the total available surface area and active sites for adsorption of the adsorbent [8]. However, the adsorption capacity decreases with increase in the adsorbent amount; at higher amount, there may be overlapping occurs in available surface area

so the total effective surface may decrease or there may be unsaturated active sites on the surface of adsorbent [28].

3.4. Effect of pH

The pH of dye solution plays an important role particularly on the adsorption capacity by influencing the chemistry of both dye molecules and adsorbent in aqueous solution. Fig. 6 shows that effect of pH on the adsorption capacity of MG has been evaluated within the pH range of 2.0–10.0 at initial dye concentration of 100 mg L<sup>-1</sup> and amount of adsorbent of 0.5 g. The highest adsorption capacity 19.65 mg g<sup>-1</sup> with 98.25% removal efficiency has been found at pH 10.0. It has been observed that uptake capacity decreased sharply as the pH of the solution decreased from 8.0 to 2.0. The minimum adsorption capacity of 15.5 mg g<sup>-1</sup> with 77.50% is measured

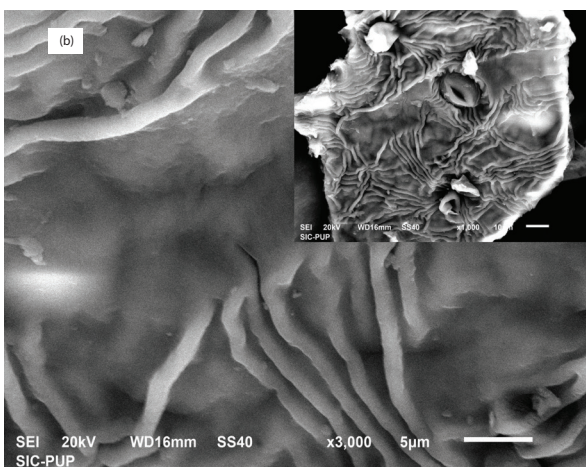
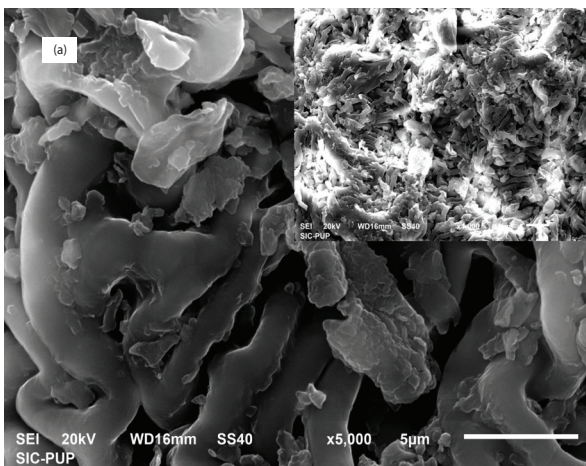


Fig. 3. SEM images of: (a) DPCP before adsorption and (b) dye adsorbed onto DPCP after 60 min dye adsorption process.

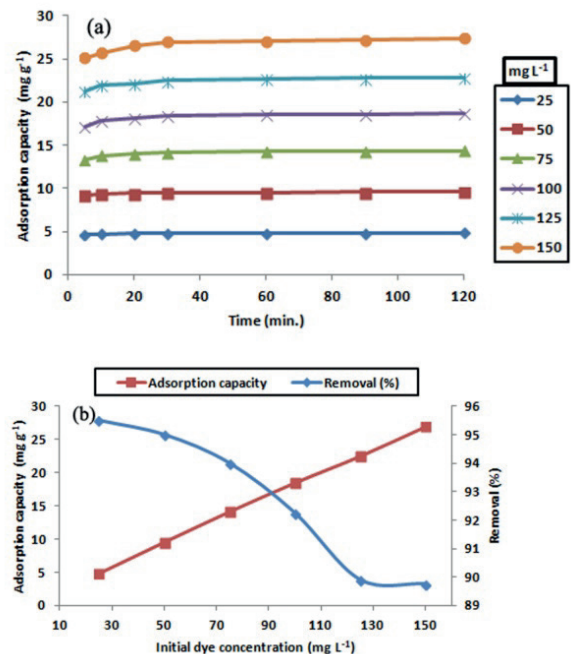


Fig. 4. Variation of: (a) adsorption capacity (mg g<sup>-1</sup>) as a function of contact time at different initial MG concentrations and (b) percentage removal and adsorption capacity (mg g<sup>-1</sup>) of MG with different initial dye concentrations of MG.

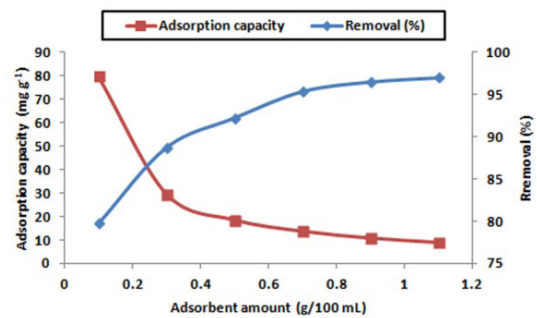


Fig. 5. Variation of MG removal and adsorption capacity (mg g<sup>-1</sup>) as a function of adsorbent amount.

at pH 2.0. XRF studies show that cellulose is main constituent of DPCP. Thus, DPCP contain hydroxyl group, which has tendency to form hydrogen bond with both proton as well as hydrogen ion. As a result in acidic medium, surface of DPCP get protonated and there is electrostatic repulsion arise between adsorbent and cationic dye in acidic medium, which in alkaline medium there is more affinity of adsorbent toward cationic dye.

### 3.5. Effect of ionic strength

Adsorption process can be affected in the presence of some metal ions, which are presented in wastewaters as ionic strength. The electrostatic attraction mechanism of cationic dyes in high ionic strength solutions has been suppressed due to the competition with the Na<sup>+</sup> for the active sites on adsorbent surface, leading to electrostatic repulsion [29]. Fig. 7 narrates the effect of varying the concentration of NaCl on the adsorption of MG by DPCP. It has been observed that the adsorption of MG slightly decreases as the NaCl concentration increases. At high salt concentration, this reduction in dye suggested that electrostatic interaction is not only the major force of interaction but also the hydrophobic-hydrophobic interaction and other forces [4].

### 3.6. Adsorption kinetics

The kinetic analysis is a very important tool for understanding the treatment of aqueous solutions that provides

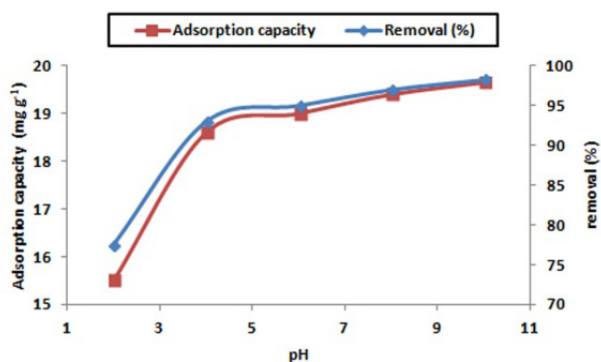


Fig. 6. Variation of adsorption capacity (mg g<sup>-1</sup>) and percentage removal of MG with initial solution pH.

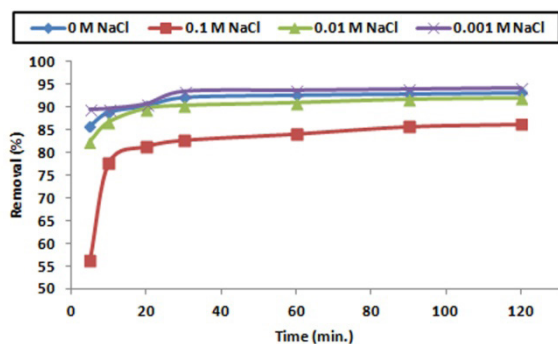


Fig. 7. Variation of ionic strength on the adsorption of MG onto DPCP.

valuable information regarding the controlling mechanisms of the adsorption process. Kinetic studies have been performed for adsorption of MG dye onto DPCP to explore the adsorption mechanism. Four kinetic models: pseudo-first-order (Eq. (3)), pseudo-second-order (Eq. (4)), Weber–Morris intra-particle diffusion (Eq. (5)) and Elovich (Eq. (6)) have been used in this study [30–32] as follows:

$$\log(q_e - q_t) = \log q_e - k_1 t / 2.303 \quad (3)$$

$$t / q_t = 1 / (k_2 q_e^2) + t / q_e \quad (4)$$

$$q_t = k_{ipd} t^{1/2} + C \quad (5)$$

$$q_t = 1 / \beta \ln(\alpha \beta) + 1 / \beta \ln t \quad (6)$$

where  $q_e$  and  $q_t$  are the amount of dye adsorbed at equilibrium and at any time  $t$  (mg g<sup>-1</sup>), respectively;  $k_1$  (min<sup>-1</sup>),  $k_2$  (g mg<sup>-1</sup> min<sup>-1</sup>) and  $k_{ipd}$  (mg g<sup>-1</sup> min<sup>-1/2</sup>) are the rate constants of adsorption for pseudo-first-order model, pseudo-second-order model and intra-particle diffusion, respectively;  $C$  (mg g<sup>-1</sup>),  $\alpha$  (mg g<sup>-1</sup> min<sup>-1</sup>) and  $\beta$  (g min<sup>-1</sup>) are the constants, which gives the thickness of the boundary layer, initial adsorption rate and the extent of surface coverage, respectively.

The experimental data do not give linear plot for pseudo-first-order model. It is evident from Fig. 8(a), that the experimental data have been well fitted to pseudo-second-order with a high value of correlation

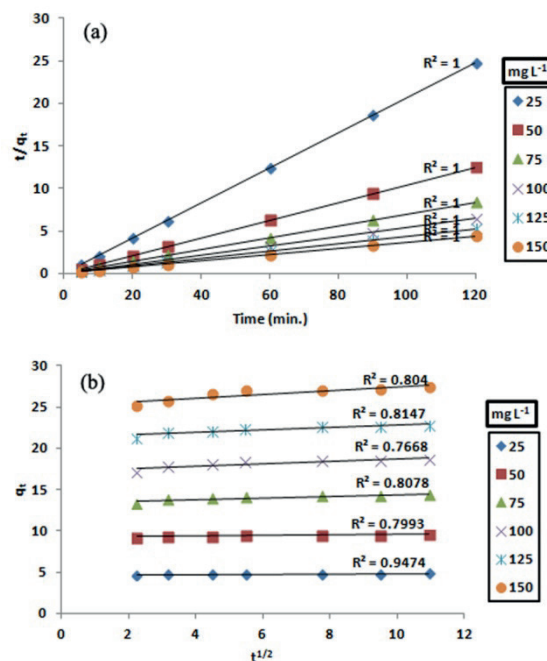


Fig. 8. At various initial MG concentrations: (a) pseudo-second-order kinetic plot and (b) intra-particle diffusion model.

coefficient ( $R^2$ : 1.000) for all initial concentrations of MG. In order to analyze the contribution of mass transport rate in the adsorption process, the data have been subjected to intra-particle diffusion model. It is clear from Fig. 8(b) that the plot between  $q_t$  vs.  $t^{1/2}$  is a linear plot but do not pass through origin. The deviation may arise from variation of mass transfer in initial and final stage. Since  $C$  is not equal to zero, thus intra-particle diffusion is the rate-controlling step [33]. The data are then subjected to Elovich equation, which basically supports chemisorptions, but are also applicable to system having heterogeneous adsorbing surface [34]. The fitness of data to Elovich model indicates that heterogeneous mechanism likely to be responsible for dye uptake. The kinetic parameters of MG removal using a fixed amount of adsorbent (0.5 g) over the initial MG concentrations in the range of 25–150 mg L<sup>-1</sup> have been represented in Table 2.

### 3.7. Adsorption isotherm

Adsorption isotherm analysis is a very effective tool to describe the equilibrium between concentrations of the adsorbate on the solid phase and concentration in liquid phase. The equilibrium adsorption process has been analyzed using Langmuir, Freundlich, Temkin and Dubinin–Radushkevich (D–R) isotherm equations.

Langmuir adsorption isotherm assumes that adsorption takes place at specific homogenous sites within adsorbent and the monolayer adsorption onto a surface containing a finite number of identical sites. The linear form of Langmuir isotherm is expressed by the following equation [35]:

$$C_e / q_e = C_e / q_m + 1 / q_m b_L \quad (7)$$

where  $C_e$  is the equilibrium dye concentration (mg L<sup>-1</sup>),  $q_e$  is the dye concentration at equilibrium onto the adsorbent (mg g<sup>-1</sup>),  $q_m$  is the dye concentration when monolayer forms on the adsorbent (mg g<sup>-1</sup>) and  $b_L$  is the Langmuir constant related to the affinity of the binding sites and energy of bio-adsorption (L mg<sup>-1</sup>). The values of  $b_L$  and  $q_m$  have been calculated from the intercept and slope of the plots  $C_e/q_e$  vs.  $C_e$  and are given in Table 3 and Fig. 9(a).

A dimensionless constant separation factor ( $R_L$ ) has been used to identify the feasibility and favorability of the adsorption process. The separation factor ( $R_L$ ) [9] is expressed by equation:

$$R_L = 1 / (1 + b_L C_0) \quad (8)$$

The value of  $R_L$  indicates the type of isotherm, i.e., favorable ( $0 < R_L < 1$ ), linear ( $R_L = 1$ ) or unfavorable ( $R_L > 1$ ). The value of  $R_L$  has been less than unity for this study and is contained in Table 3, states highly favorable adsorption for the MG and DPCP system.

Freundlich isotherm is an empirical equation based on the adsorption onto a heterogeneous surface. The linear form of Freundlich equation is represented as follows [36]:

$$\ln q_e = \ln K_F + (1/n) \ln C_e \quad (9)$$

where  $K_F$  (mg g<sup>-1</sup>) and  $n$  are the Freundlich constants, which are related to the adsorption capacity and adsorption intensity

Table 2

Kinetic parameters of reaction-based and diffusion-based models for the adsorption of MG onto DPCP at various initial MG concentrations

Models	Parameters	25 mg L <sup>-1</sup>	50 mg L <sup>-1</sup>	75 mg L <sup>-1</sup>	100 mg L <sup>-1</sup>	125 mg L <sup>-1</sup>	150 mg L <sup>-1</sup>
Pseudo-second order	$k_2$ (g mg <sup>-1</sup> min <sup>-1</sup> )	0.5228	0.3067	0.1302	0.0990	0.0864	0.0543
	$q_e$ (mg g <sup>-1</sup> )	4.8567	9.6246	14.3885	18.7266	22.8833	27.4725
	$R^2$	1.0000	1.0000	1.0000	1.0000	1.0000	1.0000
Intra-particle diffusion	$k_{ipd}$ (mg g <sup>-1</sup> min <sup>-1/2</sup> )	0.0197	0.0402	0.0970	0.1434	0.1513	0.2325
	$C$ (mg g <sup>-1</sup> )	4.6599	9.2052	13.4109	17.2976	21.3553	25.0863
	$R^2$	0.9474	0.7993	0.8078	0.7668	0.8147	0.8040
Elovich	$\alpha$ (mg g <sup>-1</sup> min <sup>-1</sup> )	$4.31 \times 10^{37}$	$2.94 \times 10^{31}$	$6.48 \times 10^{18}$	$1.63 \times 10^{16}$	$3.11 \times 10^{19}$	$6.54 \times 10^{14}$
	$B$ (g min <sup>-1</sup> )	19.4932	8.2440	3.4199	2.2836	2.2002	1.4267
	$R^2$	0.9890	0.9247	0.9353	0.9120	0.9368	0.9317

Table 3

Isotherm constants for the adsorption of MG onto DPCP at various initial MG concentrations

Isotherm	Isotherm constants			
Langmuir	$q_m$ (mg g <sup>-1</sup> )	$b_L$ (L mg <sup>-1</sup> )	$R_L$	$R^2$
	39.2157	0.1222	0.0517–0.2466	0.9801
Freundlich	$n$	$K_F$ (mg g <sup>-1</sup> )		$R^2$
	1.5850	39.2645		0.9823
Temkin	$\alpha$ (L g <sup>-1</sup> )	$\beta$ (mg L <sup>-1</sup> )	$b$ (J mg <sup>-1</sup> )	$R^2$
	2.1493	8.1216	310.3316	0.9767
Dubinin–Radushkevich	$q_D$ (mg g <sup>-1</sup> )	$B$ (mol <sup>2</sup> J <sup>-2</sup> )	$E$ (kJ mol <sup>-1</sup> )	$R^2$
	27.5857	$5.5 \times 10^{-4}$	0.9174	0.8694

of the system and determined from the plot of  $\ln q_e$  vs.  $\ln C_e$  and are given in Table 3 and Fig. 9(b). The value of  $n$  (i.e.,  $>1$ ) has been indicated the favorable and heterogeneous nature of adsorption.

Temkin isotherm has been considered for the effects of indirect adsorbate–adsorbent interactions and the linear form of Temkin [37] relationship is given as:

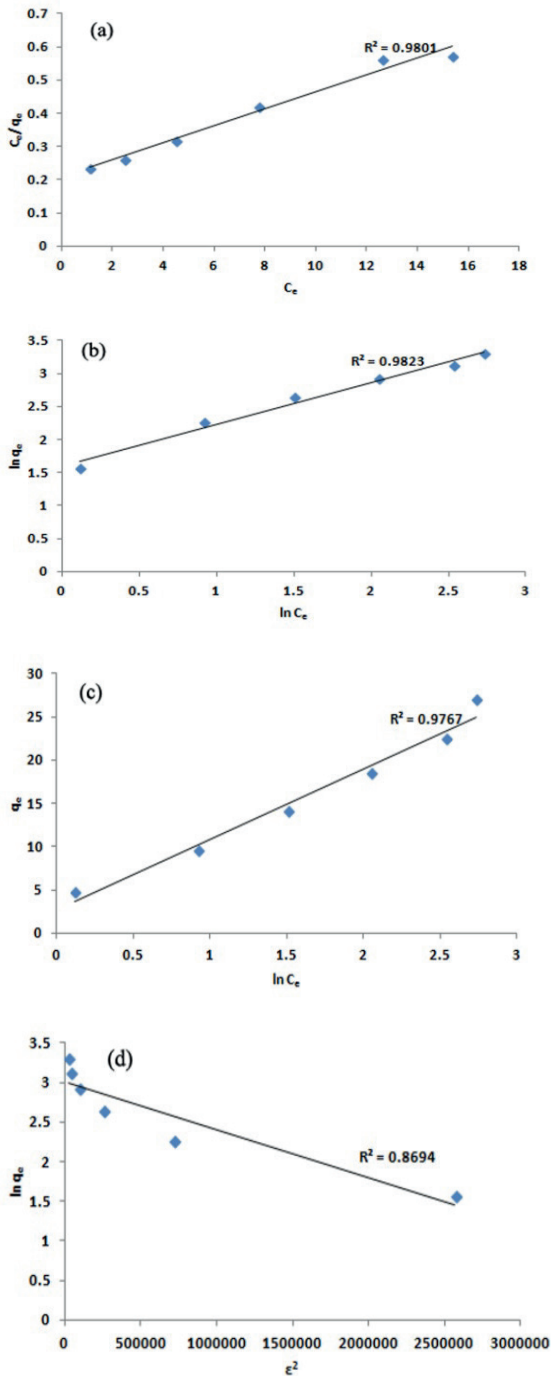


Fig. 9. Isotherm plots: Langmuir isotherm (a), Freundlich isotherm (b), Temkin isotherm (c) and Dubinin–Radushkevich isotherm (d).

$$q_e = \beta \ln \alpha + \beta \ln C_e \tag{10}$$

where  $\beta = (RT)/b$ :

where  $T$  is the absolute temperature in Kelvin,  $R$  is the universal constant and  $b$  is Temkin constant related to heat of adsorption ( $\text{J mg}^{-1}$ ). Temkin constants  $\alpha$  and  $\beta$  have been calculated from the slope and intercept of  $q_e$  vs.  $\ln C_e$  (Table 3, Fig. 9(c)).

Dubinin–Radushkevich (D–R) isotherm is dependent on temperature and is employed for the prediction of whether the adsorption process is physical or chemical in nature by evaluating the apparent mean free energy of the adsorption process. D–R linearized equation and Polanyi potential are illustrated as follows [38]:

$$\ln q_e = \ln q_D - B\epsilon^2 \tag{11}$$

$$\epsilon = RT \ln(1 + 1/C_e) \tag{12}$$

where  $B$  is a constant related to the mean free energy of adsorption ( $\text{mol}^2 \text{J}^{-2}$ ) and  $q_D$  is the theoretical saturation capacity ( $\text{mg g}^{-1}$ ). The values of  $B$  and  $q_D$  have been calculated from intercept and slope of the plots  $\ln q_e$  vs.  $\epsilon^2$  (Fig. 9(d)). The mean free energy  $E$  of adsorption per molecule of adsorbate has been calculated from equation:

$$E = 1/(2B)^{0.5} \tag{13}$$

The adsorption isotherms are useful to describe the interaction between adsorbate and adsorbent of any system, which provides the information about mechanism, the surface properties and affinities of the adsorbent. In terms of  $R^2$  values, Freundlich isotherm gave out the highest value for adsorption of MG dye (0.9823), followed by Langmuir (0.9801), Temkin (0.9767) and D–R (0.8694). Of all the models D–R model, which does not assume a homogeneous surface or a constant biosorption potential as Langmuir model, so it is least fitting with low  $R^2$  value. Hence, based on this analysis, Langmuir model, which predicts a monolayer adsorption process with higher  $R^2$  (the adsorption of dye occurs through strong interactions, electrostatic or hydrogen bonding) is the better model as compared with D–R model to describe the adsorption of MG. Similar results have been reported by other researchers [8,39]. Adsorption of Langmuir maximum adsorption capacity ( $q_m$ ) for MG onto DPCP is  $39.22 \text{ mg g}^{-1}$ . Table 4 shows the comparison of the maximum adsorption capacity ( $q_m$ ) of various adsorbents on the adsorption of MG. The adsorption capacity of DPCP has been found to be extremely good as compared with other adsorbents reported in the literature [40–48].

### 3.8. Thermodynamic studies

The effect of temperature on the adsorption of MG onto DPCP has been carried out for  $100 \text{ mg L}^{-1}$  initial dye concentration at different temperature (293.15, 303.15, 313.15 and 323.15 K) using 0.5 g of DPCP. The experimental results

indicate that adsorption capacity increases with rise in temperature, i.e., the process is endothermic in nature. The thermodynamic parameters such as change in free energy ( $\Delta G$ ), enthalpy change ( $\Delta H$ ) and entropy change ( $\Delta S$ ) have been calculated at different temperature using the following equations [11]:

$$\Delta G = -2.303RT \log K_D \quad (14)$$

$$K_D = q_e / C_e \quad (15)$$

Table 4  
Comparison of adsorption capacities of MG on various adsorbents

S.No.	Name of adsorbent	$q_{\max}$ (mg g <sup>-1</sup> )	References
1	Peat	143.70	[40]
2	Chemically modified <i>Azolla pinnata</i>	87.00	[41]
3	<i>Artocarpus altilis</i> (breadfruit)	55.30	[42]
4	DPCP	39.22	Present study
5	Rubber wood sawdust	36.45	[43]
6	Almond shell ( <i>Prunus dulcis</i> )	29.00	[44]
7	Natural zeolite	25.14	[45]
8	<i>Borassus</i> bark	20.70	[46]
9	<i>Arundo donax</i> root	8.49	[47]
10	Hen feather	2.82	[48]

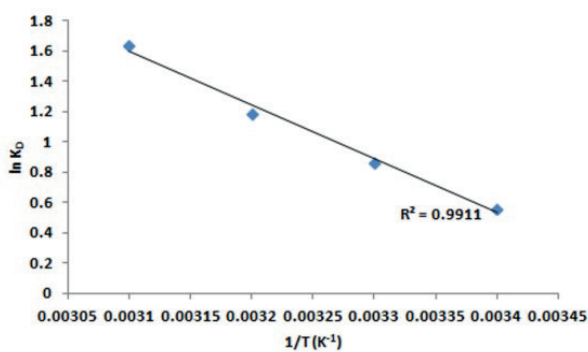


Fig. 10. Van't Hoff plot for the determination of thermodynamics parameters.

Table 5  
Thermodynamic parameters for MG onto DPCP

Temperature (K)	$K_D$	$\Delta G$ (kJ mol <sup>-1</sup> )	$\Delta H$ (kJ mol <sup>-1</sup> )	$\Delta S$ (J mol <sup>-1</sup> K <sup>-1</sup> )
293.15	1.7512	-1.3656	29.4823	104.6525
303.15	2.3806	-2.1862		
313.15	3.2783	-3.0912		
323.15	5.1333	-4.3946		

Also:

$$\Delta G = \Delta H - T\Delta S \quad (16)$$

$$\ln K_D = \Delta S / R - \Delta H / RT \quad (17)$$

where  $R$  is the universal gas constant (8.314 J mol<sup>-1</sup> K<sup>-1</sup>) and  $K_D$  is the distribution coefficient for the adsorption (K g<sup>-1</sup>). The values of  $\Delta H$  and  $\Delta S$  have been calculated from slope and intercept of the plot of  $\ln K_D$  vs.  $1/T$  (Fig. 10) and are given in Table 5. The negative values of  $\Delta G$  have been indicated the feasibility of the system. The low value of  $\Delta H$  supports the physisorption. The positive  $\Delta S$  (104.6525 J mol<sup>-1</sup> K<sup>-1</sup>) reflects the increase in randomness at the adsorbate at the solid-liquid interface, which occurs due to desorption of water molecules from adsorbent surface during the process of adsorption [4].

### 3.9. Desorption study

Regeneration of the adsorbent makes the process economical. At the optimized conditions of the experiment the adsorbent has been separated and washed with desorption media (1% HCl, NaOH or CH<sub>3</sub>COOH). From experimental data, NaOH has been found to be an effective desorption medium with the maximum efficiency (Fig. 11(a)). After six cycles, the adsorption efficiency of DPCP has been lowered to 67.13% from 98.13% (Fig. 11(b)). As the regenerated

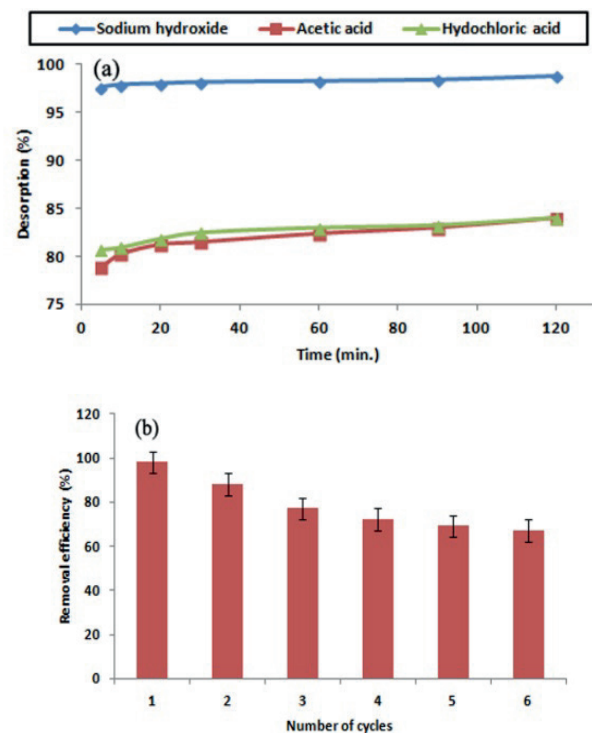


Fig. 11. Desorption studies of MG from adsorbent: (a) using different eluting solvents and (b) recycling efficiency cycles with sodium hydroxide solution as desorbing agent.

adsorbent provided the satisfactory adsorption capability results toward MG dye, it can be used as a potential adsorbent for the effluent treatment.

#### 4. Conclusion

The results obtained in the present study confirm that DPCP without any pre-treatment can be readily used as an effective adsorbent for the removal of MG from aqueous solution. The effects of different parameters have been systematically investigated. The adsorbent shows a good adsorption capacity toward the adsorption of MG without any activation or pre-treatment, in short equilibrium time (60 min). The classification of the equilibrium data according to simulation of the adsorption behavior is: Freundlich > Langmuir > Temkin > D–R. The kinetic studies indicated that the suitability of pseudo-second-order model with intra-particle diffusion as rate controlling step. Thermodynamic studies have been confirmed that the adsorption system is endothermic, physisorption and feasible in nature. DPCP has been successfully regenerated with NaOH and retained its good adsorption capacity. Fast kinetics with a high adsorption capacity make DPCP attractive and great advantages in wastewater remediation as it would be economical and energy saving.

#### Acknowledgment

Authors acknowledge sincere thanks to UGC, New Delhi for awarding the UGC-BSR Fellowship (to Ms. Rajvir Kaur) for carrying out the research work successfully.

#### Symbols

$t$	—	Contact time, min
$T$	—	Temperature, K
$V$	—	Volume of solution, L
$W$	—	Mass of dry adsorbent, g
$C_0$	—	Initial concentration of MG, mg L <sup>-1</sup>
$C_e$	—	Equilibrium concentration, mg L <sup>-1</sup>
$q_t$	—	Adsorption capacity of MG at any time $t$ , mg g <sup>-1</sup>
$q_e$	—	Adsorption capacity of MG at equilibrium, mg g <sup>-1</sup>
$k_1$	—	Pseudo-first-order rate constant, min <sup>-1</sup>
$k_2$	—	Pseudo-second-order rate constant, g mg <sup>-1</sup> min <sup>-1</sup>
$k_{ipd}$	—	Intra-particle diffusion rate constant, mg g <sup>-1</sup> min <sup>-1/2</sup>
$C$	—	Thickness of the boundary layer, mg g <sup>-1</sup>
$\alpha$	—	Initial adsorption rate, mg g <sup>-1</sup> min <sup>-1</sup>
$\beta$	—	The extent of surface coverage, g min <sup>-1</sup>
$q_m$	—	Monolayer adsorption capacity, mg g <sup>-1</sup>
$b_L$	—	Langmuir constant, L mg <sup>-1</sup>
$R_L$	—	Separation factor, dimensionless
$K_F$	—	Freundlich constant, mg g <sup>-1</sup>
$1/n$	—	Heterogeneity factor, dimensionless
$b$	—	Temkin constant related to heat of adsorption, J mg <sup>-1</sup>
$B$	—	Mean free energy of adsorption, mol <sup>2</sup> J <sup>-2</sup>
$q_D$	—	Theoretical saturation capacity, mg g <sup>-1</sup>

$R$	—	Universal gas constant, J mol <sup>-1</sup> K <sup>-1</sup>
$R^2$	—	Linear correlation coefficient
$\Delta G$	—	Gibbs free energy change, kJ mol <sup>-1</sup>
$\Delta H$	—	Enthalpy change, kJ mol <sup>-1</sup>
$\Delta S$	—	Entropy change, J mol <sup>-1</sup> K <sup>-1</sup>

#### References

- [1] A.K. Meena, A. Yadav, M.M. Rao, Ayurvedic uses and pharmacological activities of *Calotropis procera* Linn, Asian J. Tradit. Med., 6 (2011) 45–53.
- [2] S.K. Kapur, Y.K. Sarin, Medico-botanical survey of medicinal and aromatic plants of Katra valley (J.K. State), India, Indian Drugs, 22 (1984) 4–10.
- [3] R. Kaur, H. Kaur, Electrochemical degradation of Congo red from aqueous solution: role of graphite anode as electrode material, Port. Electrochim. Acta, 34 (2016) 185–196.
- [4] M.K. Dahri, M.R.R. Kooh, L.B.L. Lim, Application of *Casuarina equisetifolia* needle for the removal of methylene blue and malachite green dyes from aqueous solution, Alexandria Eng. J., 54 (2015) 1253–1263.
- [5] M.A. Ahmed, R. Alrozi, Removal of malachite green dye from aqueous solution using rambutan peel-based activated carbon: equilibrium, kinetic and thermodynamic studies, Chem. Eng. J., 171 (2011) 510–516.
- [6] M.E. Yonar, S.M. Yonar, Changes in selected immunological parameters and antioxidant status of rainbow trout exposed to malachite green (*Oncorhynchus mykiss*, Walbaum, 1792), Pestic. Biochem. Physiol., 97 (2010) 19–23.
- [7] S. Coruh, S. Eleveli, Optimization of malachite green dye removal by sepiolite clay using a central composite design, Global NEST J., 16 (2014) 339–347.
- [8] N. Boudechiche, H. Mokaddem, Z. Sadaoui, Biosorption of cationic dye from aqueous solutions onto lignocellulosic biomass (*Luffa cylindrica*): characterization, equilibrium, kinetic and thermodynamic studies, Int. J. Ind. Chem., 7 (2016) 167–180.
- [9] G.S. Dawood, Removal Orange (G) dye from aqueous solution by adsorption on bentonite, Tikrit J. Pure Sci., 15 (2010) 231–234.
- [10] H. Kaur, Swati, R. Kaur, Kinetic and isotherm studies of congo red adsorption from aqueous solution by biowaste material, Chem. Sci. Trans., 3 (2014) 1300–1309.
- [11] R. Kaur, H. Kaur, Adsorption of Amido Black 10B from aqueous solution using weed waste as adsorbent: characterization, equilibrium, kinetic and thermodynamic studies, Asian J. Chem., 29 (2017) 441–446.
- [12] A. Thakur, H. Kaur, Paper industry waste sludge: a low-cost adsorbent for removal of Malachite green dye, Asian J. Chem., 28 (2016) 2139–2145.
- [13] K. Belay, M. Abebe, Removal of Malachite Green from aqueous solutions by adsorption using low cost Biosorbent Neem Leaf (*Azadirachta indica*), Merit Res. J. Environ. Sci. Toxicol., 2 (2014) 86–92.
- [14] E.O. Oyelude, F.A. Takyi, Removal of methylene blue from aqueous solution using alkali-modified malted sorghum mash, Turkish J. Eng. Environ. Sci., 36 (2012) 161–169.
- [15] S. Chowdhury, R. Mishra, P. Saha, P. Kushwaha, Adsorption thermodynamics, kinetics and isosteric heat of adsorption of malachite green onto chemically modified rice husk, Desalination, 265 (2011) 159–168.
- [16] E. Akar, A. Altinişik, Y. Seki, Using of activated carbon produced from spent tea leaves for the removal of malachite green from aqueous solution, Ecol. Eng., 52 (2013) 19–27.
- [17] H.I. Cheing, L.B.L. Lim, N. Priyantha, Enhancing adsorption capacity of toxic malachite green dye through chemically modified breadnut peel: equilibrium, thermodynamics, kinetics and regeneration studies, Environ. Technol., 36 (2015) 86–97.
- [18] M.K. Dahri, M.R.R. Kooh, L.B.L. Lim, Water remediation using low cost adsorbent walnut shell for removal of malachite green: equilibrium, kinetics, thermodynamic and regeneration studies, J. Environ. Chem. Eng., 2 (2014) 1434–1444.

- [19] B.H. Hameed, M.I. El-Khaiary, Equilibrium, kinetics and mechanism of malachite green adsorption on activated carbon prepared from bamboo by  $K_2CO_3$  activation and subsequent gasification with  $CO_2$ , *J. Hazard. Mater.*, 157 (2008) 344–351.
- [20] L.B.L. Lim, N. Priyantha, H.I. Chieng, M.K. Dahri, D.T.B. Tennakoon, T. Zehra, M. Suklueng, *Artocarpus odoratissimus* skin as a potential low-cost biosorbent for the removal of methylene blue and methyl violet 2B, *Desal. Wat. Treat.*, 53 (2015) 964–975.
- [21] L.B.L. Lim, N. Priyantha, H.I. Chieng, M.K. Dahri, *Artocarpus camansi* blanco (Breadnut) core as low-cost adsorbent for the removal of methylene blue: equilibrium, thermodynamic and kinetic studies, *Desal. Wat. Treat.*, 57 (2016) 5673–5685.
- [22] D.K. Mahmoud, M.A.M. Salleh, W.A.W.A. Karim, A. Idris, Z.Z. Abidin, Batch adsorption of basic dye using acid treated kenaf fibre char: equilibrium, kinetic and thermodynamic studies, *Chem. Eng. J.*, 181–182 (2012) 449–457.
- [23] D.R. Mulinari, H.J.C. Voorwald, M.O.H. Cioffi, G.J. Rocha, M.L.C.P. Da Silva, Surface modification of sugarcane bagasse cellulose and its effect on mechanical and water absorption properties of sugarcane bagasse cellulose/HDPE composite, *Bioresources*, 5 (2010) 661–671.
- [24] M. Eddebbagh, A. Abourriche, M. Berrada, M.B. Zina, A. Bennamara, Adsorbent material from pomegranate (*Punica granatum*) leaves: optimization on removal of methylene blue using response surface methodology, *J. Mater. Environ. Sci.*, 7 (2016) 2021–2033.
- [25] H.D. Utomo, R.Y.N. Phoon, Z. Shen, L.H. Ng, Z.B. Lim, Removal of methylene blue using chemically modified sugarcane bagasse, *Nat. Resour.*, 6 (2015) 209–220.
- [26] A. Debnath, M. Majumder, M. Pal, N.S. Das, K.K. Chattopadhyay, B. Saha, Enhanced adsorption of hexavalent chromium onto magnetic calcium ferrite nanoparticles: kinetic, isotherm and neural network modeling, *J. Dispersion Sci. Technol.*, 37 (2016) 1806–1818.
- [27] J. Iqbal, F.H. Wattoo, M.H.S. Wattoo, R. Malik, S.A. Tirmizi, M. Imran, A.B. Ghangro, Adsorption of acid yellow dye on flakes of chitosan prepared from fishery waste, *Arabian J. Chem.*, 4 (2011) 389–395.
- [28] A. Maleki, B. Hayati, M. Naghizadeh, S.W. Joo, Adsorption of hexavalent chromium by metal organic frameworks from aqueous solution, *J. Ind. Eng. Chem.*, 28 (2015) 211–216.
- [29] Y. Hu, T. Guo, X. Ye, Q. Li, M. Guo, H. Liu, Z. Wu, Dye adsorption by resins: effect of ionic strength on hydrophobic and electrostatic interactions, *Chem. Eng. J.*, 228 (2013) 392–397.
- [30] S. Lagergren, About the theory of adsorption of soluble substances, *kungliga Svenska Vetenskapsakademiens, Handle*, 24 (1898) 1–39.
- [31] Y.S. Ho, G. McKay, The kinetics of sorption of divalent metal ions onto sphagnum moss peat, *Water Res.*, 34 (2000) 735–742.
- [32] W.J. Weber, J.C. Morris, Kinetic of adsorption on carbon from solution, *J. Sanit. Eng. Div.*, 89 (1963) 31–59.
- [33] K.V. Kumar, A. Kumaran, Removal of methylene blue by mango seed kernel powder, *Biochem. Eng. J.*, 27 (2005) 83–93.
- [34] C.W. Cheung, J.F. Porter, G. McKay, Elovich equation and modified second order equation for sorption of cadmium ions onto bone char, *J. Chem. Technol. Biotechnol.*, 75 (2000) 963–970.
- [35] I. Langmuir, The adsorption of gases on plane surfaces of glass, mica and platinum, *J. Am. Chem. Soc.*, 40 (1918) 1361–1403.
- [36] H.M.F. Freundlich, Over the adsorption in solution, *J. Phys. Chem.*, 57A (1906) 385–470.
- [37] N. Barka, K. Ouzaouit, M. Abdennouri, M. El Makhfouk, Dried prickly pear cactus (*Opuntia ficus indica*) cladodes as a low-cost and eco-friendly biosorbent for dyes removal from aqueous solutions, *J. Taiwan Inst. Chem. Eng.*, 44 (2013) 52–60.
- [38] M.M. Dubinin, The potential theory of adsorption of gases and vapors for adsorbents with energetically non-uniform surface, *Chem. Rev.*, 60 (1960) 235–266.
- [39] L.B.L. Lim, N. Priyantha, D.T.B. Tennakoon, H.I. Chieng, M.K. Dahri, M. Suklueng, Breadnut peel as a highly effective low-cost biosorbent for methylene blue: equilibrium, thermodynamic and kinetic studies, *Arabian J. Chem.*, 10 (2017) S3216–S3228. doi: 10.1016/j.arabjc.2013.12.018.
- [40] H.I. Chieng, T. Zehra, L.B.L. Lim, N. Priyantha, D.T.B. Tennakoon, Sorption characteristics of peat of Brunei Darussalam IV: equilibrium, thermodynamics and kinetics of adsorption of methylene blue and malachite green dyes from aqueous solution, *Environ. Earth Sci.*, 72 (2014) 2263–2277.
- [41] M.R.R. Kooh, L.B.L. Lim, L.H. Lim, J.M.R.S. Bandara, Batch adsorption studies on the removal of malachite green from water by chemically modified *Azolla pinnata*, *Desal. Wat. Treat.*, 57 (2016) 14632–14646.
- [42] L.B.L. Lim, N. Priyantha, N.H.M. Mansor, Utilizing *Artocarpus altilis* (breadfruit) skin for the removal of malachite green: isotherm, kinetics, regeneration, and column studies, *Desal. Wat. Treat.*, 57 (2016) 16601–16610.
- [43] K.V. Kumar, S. Sivanesan, Isotherms for Malachite Green onto rubber wood (*Hevea brasiliensis*) sawdust: comparison of linear and non-linear methods, *Dyes Pigm.*, 72 (2007) 124–129.
- [44] D. Ozdes, A. Gundogdu, C. Duran, H.B. Senturk, Evaluation of adsorption characteristics of malachite green onto almond shell (*Prunus dulcis*), *Sep. Sci. Technol.*, 45 (2010) 2076–2085.
- [45] R. Han, Y. Wang, Q. Sun, L. Wang, J. Song, X. He, C. Dou, Malachite green adsorption onto natural zeolite and reuse by microwave irradiation, *J. Hazard. Mater.*, 175 (2010) 1056–1061.
- [46] S. Arivoli, M. Hema, P.M.D. Prasath, Adsorption of malachite green onto carbon prepared from borassus bark, *Arabian J. Sci. Eng.*, 34 (2009) 31–42.
- [47] J. Zhang, Y. Li, C. Zhang, Y. Jing, Adsorption of malachite green from aqueous solution onto carbon prepared from *Arundo donax* root, *J. Hazard. Mater.*, 150 (2008) 774–782.
- [48] A. Mittal, Adsorption kinetics of removal of a toxic dye, Malachite Green, from wastewater by using hen feathers, *J. Hazard. Mater.*, 133 (2006) 196–202.